THE Ras-LIKE PROTEIN R-Ras2/TC21 IS IMPORTANT FOR PROPER MAMMARY GLAND DEVELOPMENT

by

Romain M. Larive, Antonio Abad, Clara M. Cardaba, Teresa Hernández, Marta Cañamero, Enrique de Álava, Eugenio Santos, Balbino Alarcón, and Xosé R. Bustelo

SUPPLEMENTARY INFORMATION[a]

[a]This file includes:

1. SUPPLEMENTARY TABLES

TABLE S1. Normal fertility rates in male and female *RRas2*$^{-/-}$ mice.

Crosses	Productive crosses	Number of newborns per litter	Number of litters per female
RRas2$^{+/+}$ x *RRas2*$^{+/+}$	100%	6.8 ± 0.3[a,b]	5.9 ± 0.9
RRas2$^{-/-}$ x *RRas2*$^{-/-}$	100%	6.3 ± 0.4[c]	6.2 ± 0.6

[a]Values represent the mean ± standard error of the mean. [b]*n* = 7 crosses (≥ 500 newborns). [c]*n* = 10 crosses (≥ 500 newborns)

TABLE S2. Cardiovascular parameters of 3 month-old *RRas2*$^{-/-}$ mice.

Physiological parameter	*RRas2*$^{+/+}$	*RRas2*$^{-/-}$
Systolic arterial pressure (mm Hg)	108.6 ± 3.1[a]	109.7 ± 3.5
Diastolic arterial pressure (mm Hg)	78.2 ± 1.4	78.8 ± 2.9
Mean arterial pressure (mm Hg)	88.1 ±1.9	88.8 ± 3.1
Heart rate (beats/min)	675 ± 20	684 ± 25

[a]Values represent the mean ± standard error of the mean (*n* = 5 animals/genotype)

2. SUPPLEMENTARY FIGURE LEGENDS

FIGURE S1. The absence of R-Ras2/TC21 does not impact negatively in the development of the cardiorespiratory system and adipose tissue or in the overall growth rates of mice. (**A**) Weight of hearts and lungs of *RRas2*$^{+/+}$ or *RRas2*$^{-/-}$ mice (n = 7 mice of each genotype). (**B**) Representative images of hematoxylin/eosin-stained white adipose tissue sections obtained from animals of the indicated genotypes. Scale bar, 100 μm. (**C**) Growth curves of male mice of the indicated genotypes (n = 5 mice per each genotype). Similar data were obtained with female mice.

FIGURE S2. The *RRas2* gene deficiency affects pubertal mammary gland development in animals from different genetic backgrounds. (**A**) Representative images of Carmine alum-stained mammary fat pads obtained from female mice of the indicated ages (top) and genotypes (left). Scale bars, 500 μm. One of the inguinal lymph nodes is indicated by a white asterisk (top panel in the left). (**B-E**) Quantification of the total area (B), maximal length (C), number of TEBs (D) and branching points (E) of mammary glands obtained from animals of the indicated genotypes and ages. *, $P \leq 0.05$; **, $P \leq 0.01$; ***, $P \leq 0.001$ when compared to values obtained in the appropriate wild type control (n = 5-13 animals per genotype and developmental stage).

FIGURE S3. The *RRas2* gene deficiency does not impair mammary gland outgrowth during lactancy. (**A,B**) Mammary glands obtained from mice of the indicated genotypes (A,B; left) one day after parturition were stained with either hematoxylin/eosin (A) or with antibodies to mucin (B, red color) plus DAPI (B, blue color). Scale bars, 200 μm. Mucin is expressed at the apical membrane of epithelial cells during lactation. It can be observed a similar distribution of mucin

in animals of both genotypes, suggesting that the secretory activity of the gland is not impaired in R-Ras2/TC21-deficient mice. (**C,D**) Survival (C, $n \geq 50$ pups/genotype and 7 mothers/genotype) and growth (D, $n = 5$ 21 day-old pups/genotype) rates of the offspring of wild type and *RRas2*$^{-/-}$ mothers during the first 3 weeks after birth. These studies were conducted using offsprings obtained from independently set *RRas2*$^{+/+}$ x *RRas2*$^{+/+}$ and *RRas2*$^{-/-}$ x *RRas2*$^{-/-}$ crosses

FIGURE S4. The *RRas2* gene deficiency does not alter the epithelial populations of the mammary gland. (**A,B**) Representative examples of the populations of epithelial cells present in the mammary glands of mice of the indicated genotypes according to CD24/CD29 (A) and CD24/CD49f (B) surface expression criteria. The CD24^{high}, CD24^{low} and CD24^{-} populations are enriched in luminal epithelial cells, myoepithelial/basal cells, and non-epithelial cells, respectively. The CD24^{high}+CD49f^{Low} population is enriched in mammary colony forming cells (progenitors that produce discrete colonies in low-cell density adherent two-dimensional cultures), the CD24^{medium}+CD49f^{high} population contains mammary repopulating units (mammary stem cells capable of regenerating new glands *in vivo*), and the CD24^{low}CD49f^{low} population is enriched in myoepithelial cells. The CD24^{-}/CD49f^{-} population is considered formed by non-epithelial cells. No statistically significant deviations were seen among those populations in the mammary glands of wild type and R-Ras2/TC21-deficient mice ($n = 4$ mice per genotype).

FIGURE S5. Normal budding and morphogenic processes of in vitro *RRas2*$^{-/-}$ organoids. (**A**) Representative phase-contrast images of organoids of the indicated genotypes (left) cultured in either starvation (left panels) or FGF2 supplemented (right panels) conditions. (**B**) Percentage of

organoids displaying at least three budded branches in the above conditions. *, $P<0.05$, **, $P<0.005$ relative to the values obtained with wild type organoids cultures in starvation conditions. N.S., statistically non-significant changes between the indicated experimental samples (in brackets). ($n = 3$ independent experiments, each involving at least 30 organoids). (**C**) Organoids were immunostained with antibodies to smooth muscle actin (SMA, green color), incubated with rhodamine-labeled phalloidin (to visualize the F-actin cytoskeleton, red color), and analyzed by confocal microscopy. Scale bar, 100 μm. (**D,E**) Mouse mammary epithelial cells of the indicated genotypes were assayed for migration in the absence (D) and presence (E) of collagen I as indicated in Materials and Methods ($n = 1$ experiment performed in triplicate). O.D., optical density; R.F.U., relative fluorescence units.

FIGURE S6. R-Ras2/TC21-deficient mammary epithelial cells cultured in vitro show mild defects in Erk activation in a stimulus-specific manner. **(A-D)** Cultures of mammary epithelial cells of the indicated genotypes (top) were starved for 4 h and stimulated with EGF (A), FGF2 (B), IGF (C) and HGF (D). At the indicated time points (top), total cellular lysates were obtained and subjected to immunoblot analysis with antibodies to phospho-Akt (A-D, top panels), total Akt (A-D, second panels from top), phospho-Erk (A-D, third panels from top), and total Erk (A-D, bottom panels). Similar results were obtained in 6 (A), 2 (B), 2 (C) and 2 (D) additional independent experiments.

3. SUPPLEMENTARY FIGURES

Supplementary Figure S1
Larive et al.

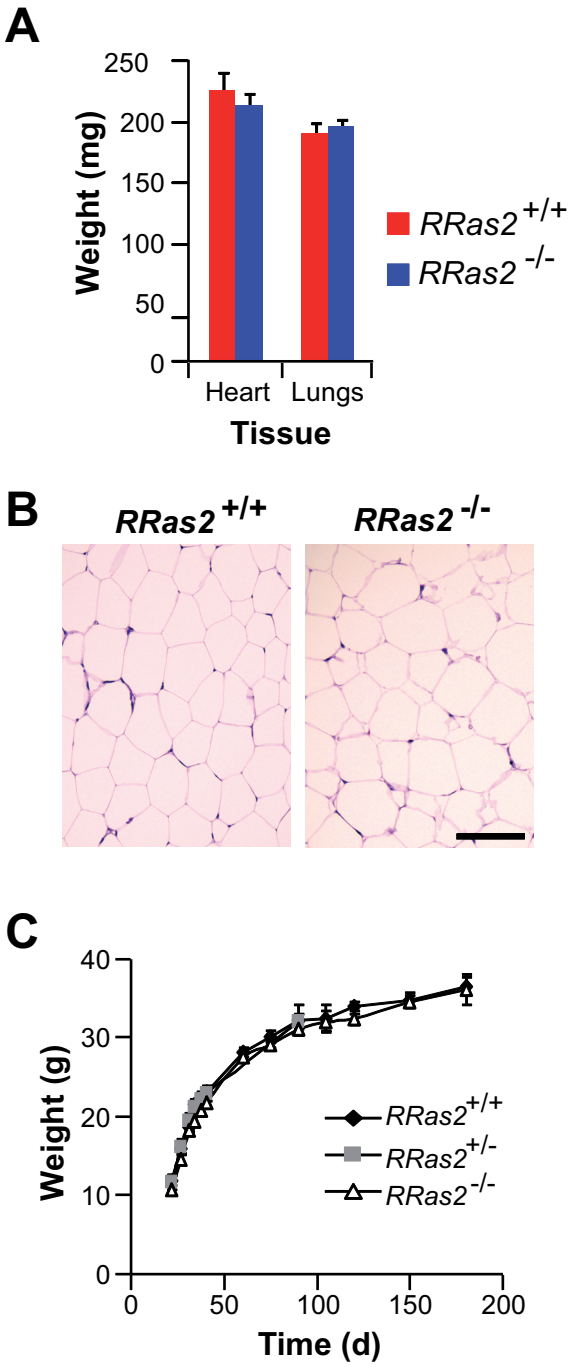

Supplementary Figure S2
Larive et al.

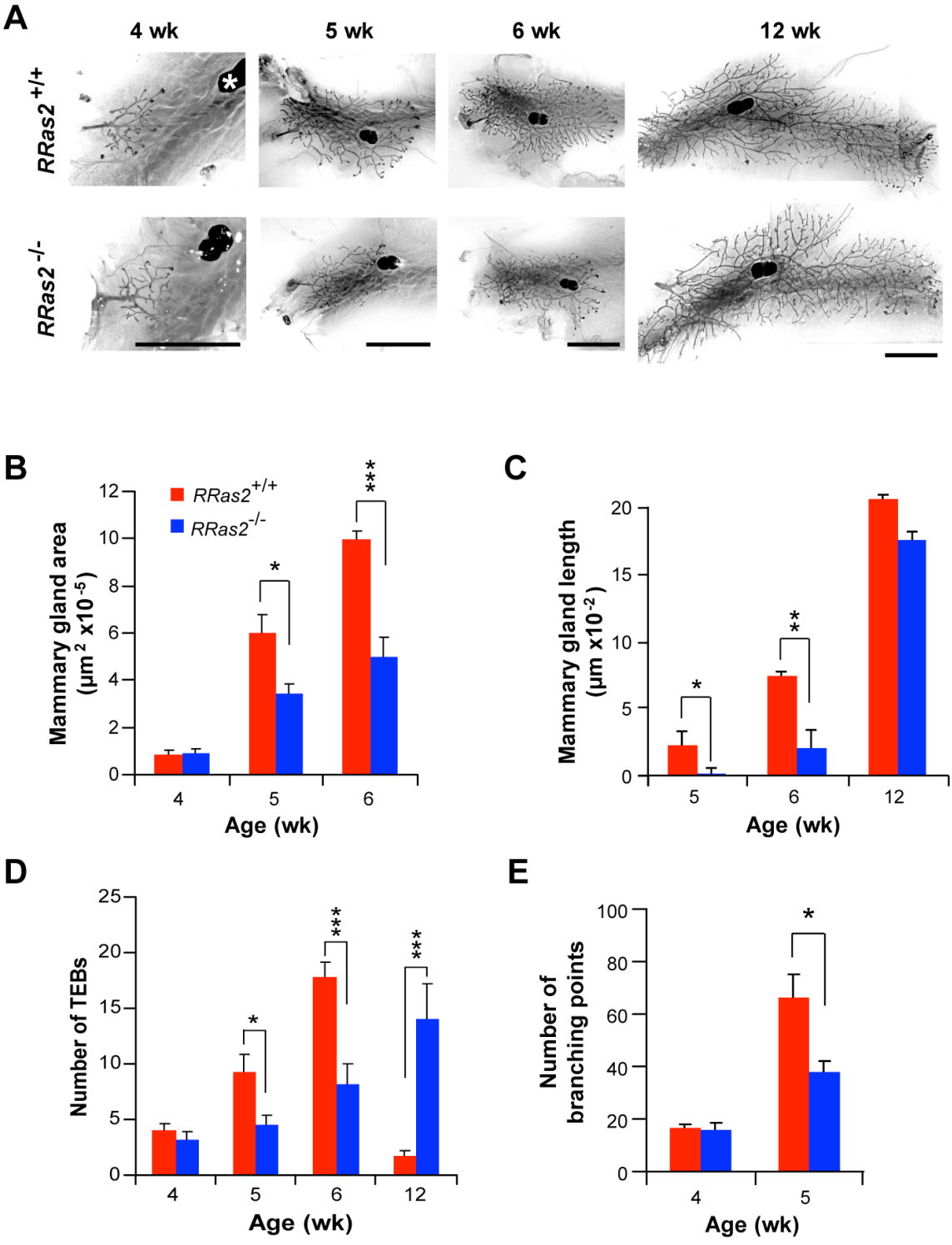

Supplementary Figure S3
Larive et al.

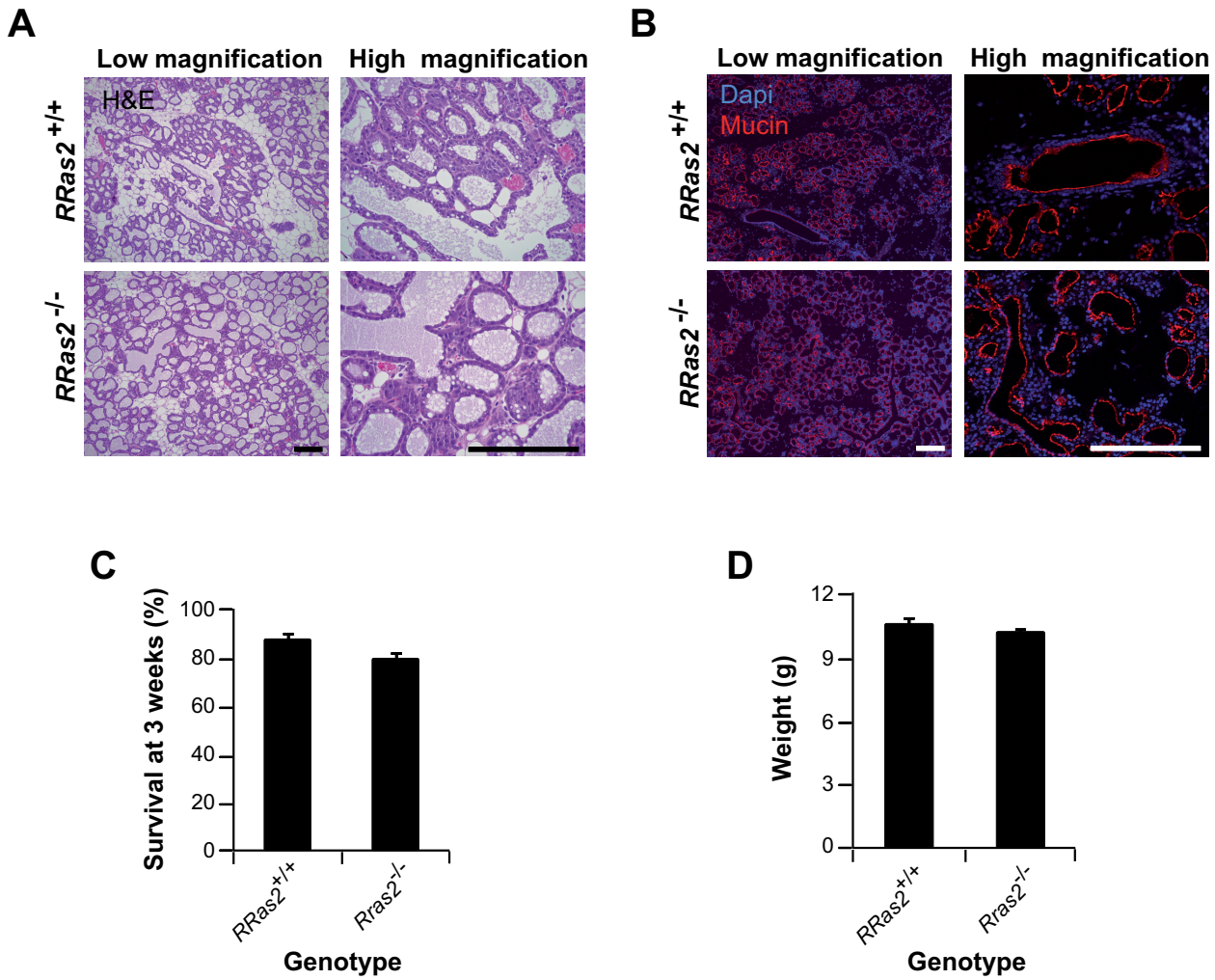

Supplementary Figure S4
Larive et al.

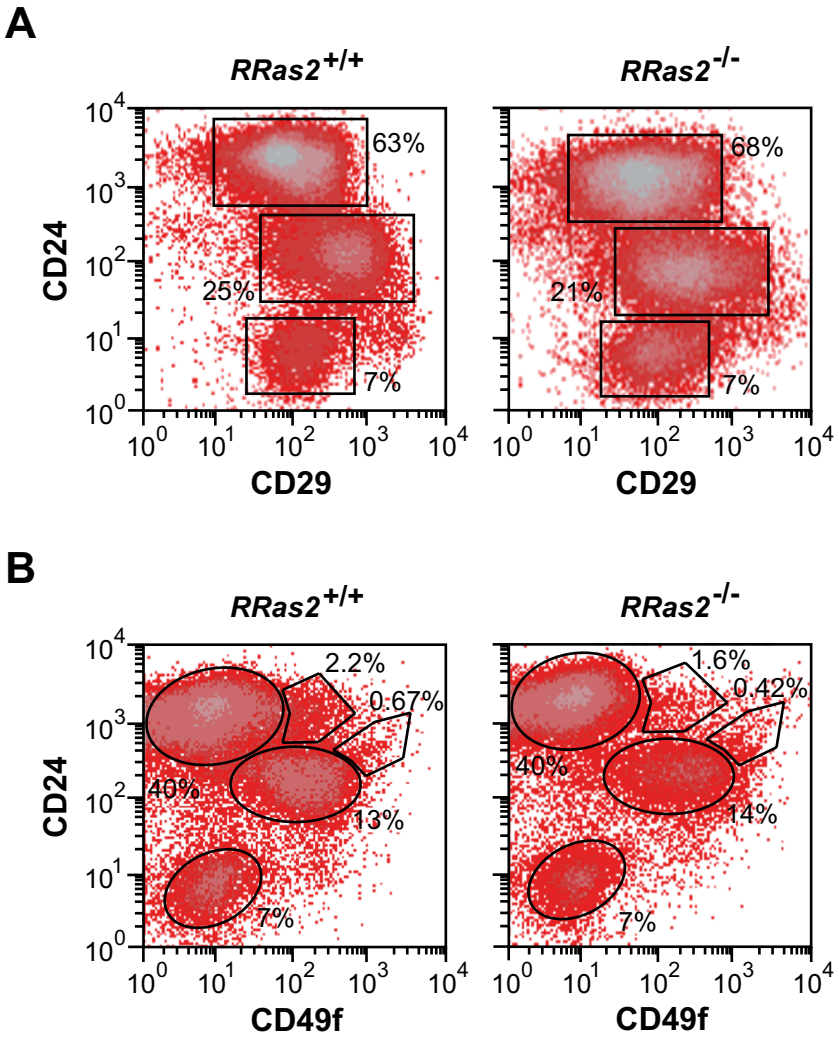

Supplementary Figure S5
Larive et al.

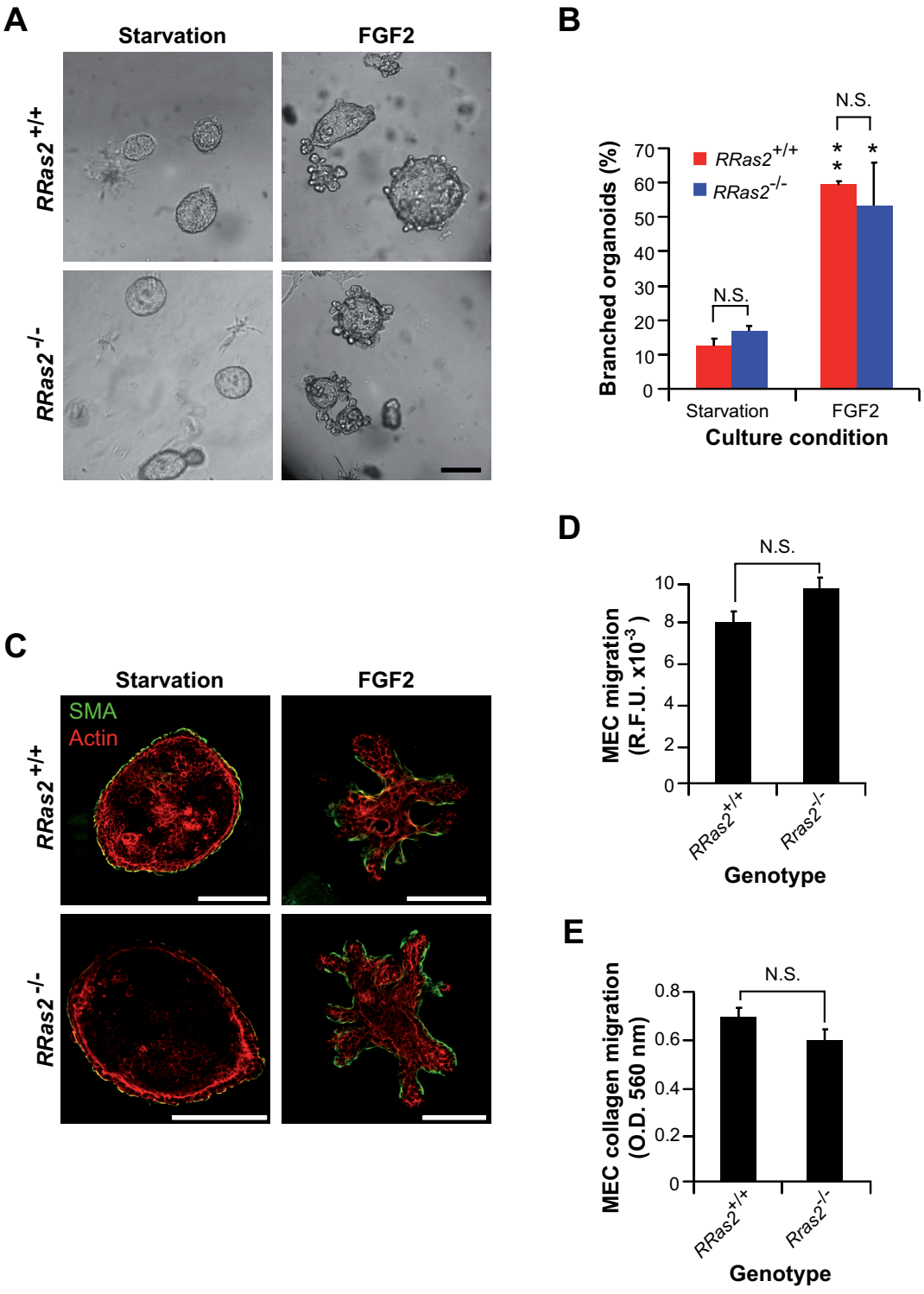

Supplementary Figure S6
Larive et al.